Wave Motion 114 (2022) 103011

Contents lists available at ScienceDirect

Wave Motion

journal homepage: www.elsevier.com/locate/wamot

Waves generated by moving loads on ice plates: Viscoelastic approximations

Evgueni Dinvay [a], Henrik Kalisch [b,*], Emilian Părău [c]

[a] INRIA Rennes Centre, Campus Universitaire de Beaulieu, 35042 Rennes Cedex, France
[b] Department of Mathematics, University of Bergen, Postbox 7800, 5020 Bergen, Norway
[c] School of Mathematics, University of East Anglia, Norwich Research Park, Norwich, NR4 7TJ, United Kingdom

ARTICLE INFO

Article history:
Received 10 December 2021
Received in revised form 7 June 2022
Accepted 10 July 2022
Available online 21 July 2022

We dedicate this article to the memory of Roger Hosking.

Keywords:
Hydro-elastic waves
Viscoelasticity
Ice sheet
Moving load
Dispersion relation

ABSTRACT

The paper investigates waves generated by the moving loads on ice plates floating on an incompressible fluid. Two different viscoelastic approximations are considered for the ice cover: A model depending on the strain-relaxation time, and a model including a hereditary delay integral. The problem is formulated in terms of the exact dispersion relation and the Dirichlet–Neumann operator connected to the fluid motion. Weakly nonlinear and linear approximations are derived by truncating the Dirichlet–Neumann operator. The Laplace transform is used to find the exact solutions of the linearized problems for the two viscoelastic models considered.

1. Introduction

The response of a floating ice sheet to moving loads is of great interest in the cold regions, where roads and airfields are sometimes built on ice (see [1]). In the vast majority of cases the ice sheet floating on the water column is modelled as a thin elastic plate, and in many of these cases, the hydroelastic (i.e. flexural-gravity) waves described by such a simplified model are in good agreement with the experiments (see [2]). Hydroelastic waves have been studied by a great number of authors, and there is now a rich literature on the subject (see e.g. [3–5] for reviews). With regards to waves excited by a moving load, following the classic works of Takizawa [6,7] and Davys et al. [8], there have been subsequent works investigating effects such wave resistance [9], compression [10] as well as the influence of deceleration [11–13], and the effect of a moving body below the ice [14]. It was also recently shown [15] that such wave patterns can be observed using satellite synthetic-aperture radar (SAR) imagery.

Most of the theoretical studies of waves generated by moving loads are considering linearized problems, which are adequate for a large range of speeds, but there are some critical speeds where they fail. Near these critical speed, nonlinear effects may be important, and there is an increasing number of papers investigating nonlinear effects near these critical speeds (e.g. [16,17]). Inspired by work on free surface water waves [18–20], some recent contributions have focussed on retaining the full dispersion relation even in the nonlinear framework [11,21], which gives very good approximations for problems where the nonlinear effect is small but nonzero.

* Corresponding author.
E-mail addresses: evgueni.dinvay@inria.fr (E. Dinvay), henrik.kalisch@uib.no (H. Kalisch), e.parau@uea.ac.uk (E. Părău).

https://doi.org/10.1016/j.wavemoti.2022.103011

A different approach to improving the thin elastic model of the ice sheet, partially motivated by experimental observations, is the inclusion of viscoelastic effects such as for example discussed in [22]. In the present paper we will concentrate on two viscoelastic models. The first model was put forward by Zhestkaya in [23], following [24] where a strain-relaxation time is included. The second model was used by Hosking et al. [25] and Wang et al. [26] and includes a memory function based on a two-parameter Boltzmann hereditary delay integral.

The two viscoelastic models will be delineated in Section 2, a weakly nonlinear approximation will be derived in Section 3, and the exact solution for the linearized problem will be obtained in Section 4. Some numerical examples will be detailed in Section 5.

2. Hydro-elastic models

We consider a three-dimensional fluid of density ρ covered by an ice plate of thickness h, under the influence of the gravitational acceleration g and with mean depth H. The Cartesian coordinates xyz are used where the horizontal x and y axes are aligned with the ice sheet, and z is the vertical coordinate. The moving load is travelling on top of the ice sheet along the x-axis. The underlying fluid is assumed to be inviscid and incompressible, and the flow is assumed irrotational. The fluid flow is described by the velocity potential $\phi(x, y, z, t)$ which satisfies the Laplace equation in the fluid domain $\{(x, y, z) \in \mathbb{R}^3 | -H < z < \eta(x, y, t)\}$

$$\nabla^2\phi = 0, \tag{2.1}$$

and by the unknown fluid surface elevation $\eta(x, y, t)$ that coincides with the vertical deformation of the lower side of the ice cover. The level $z = 0$ corresponds to the water ice interface at rest. The boundary conditions are the no-penetration condition at the bottom

$$\phi_z = 0 \quad \text{at} \quad z = -H, \tag{2.2}$$

the kinematic condition at the ice/water interface

$$\eta_t + \phi_x\eta_x + \phi_y\eta_y = \phi_z, \quad \text{at} \quad z = \eta(x, y, t), \tag{2.3}$$

and the dynamic condition at $z = \eta(x, y, t)$.

If we assume the thin linear elastic plate approximation, coupled with some form of damping quantified by a parameter b, and the density of the ice sheet is ρ_1, then it can be shown (see [2,11]) that the dynamic condition at the interface $z = \eta(x, y, t)$ is the Bernoulli equation

$$\varkappa g\Delta^2\eta - \frac{\rho_1 h^3}{12\rho}\partial_t^2\Delta\eta + \frac{\rho_1 h}{\rho}\partial_t^2\eta + \frac{b}{\rho}\partial_t\eta + g\eta + \phi_t + \frac{1}{2}|\nabla\phi|^2 + \frac{P}{\rho} = 0.$$

Here we have introduced the hydroelastic parameter $\varkappa = \mathcal{D}/(\rho g)$, where $\mathcal{D} = \frac{Eh^3}{12(1-\nu^2)}$ is the flexural rigidity of the plate, E is the Young's modulus and ν the Poisson ratio. The easiest way to take dissipation into account is to assume that the damping force is proportional to the vertical velocity. The corresponding proportionality factor $b > 0$ is assumed to be constant.

There are a couple of ways to introduce visco-elastic effects into this equation. The first is to regard the ice cover as a Kelvin–Voigt material with the strain-relaxation time τ_f. Then in the first term of the expression one substitutes $1 \to 1 + \tau_f\partial_t$. The corresponding model was studied numerically by Zhestkaya [23]. The second is to regard the ice cover as a viscoelastic material with the memory function $\Psi(t)$. Then in the first term of the expression one substitutes $\eta(t) \to \eta(t) - \int_0^\infty \Psi(\tau)\eta(t-\tau)d\tau$. The corresponding model was studied by Hosking *at al.* [25] by using Fourier transforms. Note that in both cases we still keep the 'rough' damping effects introduced via $b \geqslant 0$. The reason for this choice is that it is still necessary to take into account effects that cannot be introduced via standard viscoelastic models such as for example the influence of a snow layer atop the ice.

The main viscoelastic Bernoulli equation under consideration is

$$\mathcal{Q}\eta - \frac{\rho_1 h^3}{12\rho}\partial_t^2\Delta\eta + \frac{\rho_1 h}{\rho}\partial_t^2\eta + \frac{b}{\rho}\partial_t\eta + g\eta + \phi_t + \frac{1}{2}|\nabla\phi|^2 + \frac{P}{\rho} = 0 \tag{2.4}$$

where the bending force $\mathcal{Q}\eta$ corresponds either to the model studied by Zhestkaya [23] or to the model considered by Hosking et al. [25].

The load P is considered to be a distributed pressure

$$P(x, y, t) = \rho f(x - x_0 - vt, y) \tag{2.5}$$

moving along the x-axis at a constant speed v. Here x_0 is the initial position of the truck. Our main two examples used in the following calculations are a concentrated pressure with a delta function $f(x, y) = \gamma\delta(x, y)$ and pressure distributed uniformly over a rectangle given by $f(x, y) = \gamma\chi_{[-a_1,a_1]\times[-a_2,a_2]}(2x, 2y)/(a_1a_2)$ where γ is a loading constant parameter and $a_{1,2} > 0$. Our calculations below show that both of these loads give similar results.

3. Weakly nonlinear approximation

In most situations where flexural-gravity waves occur under field conditions, it is usually sufficient to consider the linearized problem. Indeed, in the case of ice roads and air strips, operational procedures usually adhere to very conservative estimates of the bearing capacity of the ice, and the recorded responses are generally linear. However, nonlinear flexural-gravity waves have also been observed in the field [27], and it may be desirable for a mathematical model to have the ability to describe both linear and nonlinear regimes.

Considering the ice sheet displacement $\eta(x,y,t)$ as above, we introduce the surface velocity potential $\Phi(x,y,t) = \phi(x,y,\eta(x,y,t),t)$. The unknowns η and Φ are the canonical variables fully describing the motion of the free surface of a fluid with or without a floating ice sheet. In what follows, both η and Φ are considered to be small together with their derivatives. Moreover, if we consider a large characteristic non-dimensional wavelength λ, then differentiation is given by the operator $D = (-i\partial_x, -i\partial_y) = O(1/\lambda)$, so gradients are small. We may formally define the Dirichlet–Neumann operator $G(\eta)$ by

$$G(\eta)\Phi = \left(\partial_z\phi - \partial_x\eta\partial_x\phi - \partial_y\eta\partial_y\phi\right)_{z=\eta(x,y)}. \tag{3.1}$$

The dependence of the Dirichlet–Neumann operator G on η is non-linear, but it is analytic in a certain sense [28] and can be expanded as a power series

$$G(\eta)\Phi = \sum_{j=0}^{\infty} G_j(\eta)\Phi, \tag{3.2}$$

where each operator $G_j(\eta)$ is homogeneous of degree j in η. Now the first two approximations of the Dirichlet–Neumann operator have the form

$$G_0 = |D|\tanh(H|D|), \qquad G_1(\eta) = -\partial_x\eta\partial_x - \partial_y\eta\partial_y - G_0\eta G_0,$$

where $D = (-i\partial_x, -i\partial_y)$ and $|D| = \sqrt{-\Delta} = \sqrt{-\partial_x^2 - \partial_y^2}$.

The definition of the fluid velocity together with Definition (3.1) of the Dirichlet–Neumann operator G implies

$$\eta_t = G\Phi. \tag{3.3}$$

This equation connects the functions η and Φ. To close the system, we first calculate derivatives of the potential ϕ on the surface. We need to express derivatives of ϕ in terms of derivatives of η, Φ. The gradient $\nabla\phi$ is found from the definitions of Φ and G as follows:

$$\nabla\phi = \begin{pmatrix} 1 & 0 & \eta_x \\ 0 & 1 & \eta_y \\ -\eta_x & -\eta_y & 1 \end{pmatrix}^{-1} \begin{pmatrix} \Phi_x \\ \Phi_y \\ G\Phi \end{pmatrix}. \tag{3.4}$$

Now differentiating the fluid surface potential Φ with respect to t and applying (3.3) results in

$$\Phi_t = \phi_t + \phi_z\eta_t = \phi_t + \phi_z G\Phi.$$

This together with the velocity $\nabla\phi$ from (3.4) and after disregarding terms of third and higher order gives us the acceleration potential of the inviscid fluid on surface in the form

$$\phi_t + \frac{1}{2}|\nabla\phi|^2 = \Phi_t + \frac{1}{2}\Phi_x^2 + \frac{1}{2}\Phi_y^2. \tag{3.5}$$

This expression can be substituted into Eq. (2.4) to give

$$\mathcal{Q}\eta - \frac{\rho_1 h^3}{12\rho}\partial_t^2\Delta\eta + \frac{\rho_1 h}{\rho}\partial_t^2\eta + \frac{b}{\rho}\partial_t\eta + g\eta + \Phi_t + \frac{1}{2}\Phi_x^2 + \frac{1}{2}\Phi_y^2 + \frac{P}{\rho} = 0. \tag{3.6}$$

Here the first and second derivatives of η with respect to time can be eliminated by means of Eq. (3.3) with $G = G_0 + G_1$. Indeed, truncating nonlinearity of the second order we obtain

$$\partial_t^2\eta = (G_0 + G_1(\eta))\Phi_t.$$

Now define the operator K by

$$K = 1 + \frac{\rho_1 h}{\rho}\left(1 - \frac{h^2\Delta}{12}\right)G_0, \tag{3.7}$$

with the symbol

$$K(\xi_1,\xi_2) = 1 + \frac{\rho_1 h}{\rho}\left(1 + \frac{h^2}{12}(\xi_1^2+\xi_2^2)\right)\sqrt{\xi_1^2+\xi_2^2}\tanh\left(H\sqrt{\xi_1^2+\xi_2^2}\right). \tag{3.8}$$

The fully-dispersive weakly nonlinear system for two-dimensional waves in the ice sheet is

$$\eta_t = G_0\Phi - \partial_x(\eta\Phi_x) - \partial_y(\eta\Phi_y), \tag{3.9}$$

$$\Phi_t = -\frac{g}{K}\eta - K^{-1}\mathcal{Q}\eta - \frac{b}{\rho}\frac{G_0}{K}\Phi - \Gamma - \frac{1}{2}\Phi_x^2 - \frac{1}{2}\Phi_y^2 - \frac{\rho_1 g h}{2\rho}\Delta\eta^2 + \frac{b}{\rho}\partial_x(\eta\partial_x\Phi) + \frac{b}{\rho}\partial_y(\eta\partial_y\Phi) \tag{3.10}$$

with

$$\Gamma = w - \frac{\rho_1 h}{\rho}\left(1 - \frac{h^2\Delta}{12}\right)K^{-1}G_1(\eta)w \tag{3.11}$$

and

$$w(x, y, t) = K^{-1}P/\rho$$

where the operator K and the corresponding symbol $K(\xi)$ are defined by (3.7) and (3.8). In case of the distributed moving load

$$P(x, y, t) = \rho f(x - x_0 - vt, y)$$

one finds

$$w(x, y, t) = \frac{1}{(2\pi)^2}\int_{\mathbb{R}^2}\frac{e^{i(x-x_0-vt)\xi_1+iy\xi_2}\widehat{f}(\xi_1, \xi_2)}{K(\xi_1, \xi_2)}d\xi_1 d\xi_2.$$

As it appears, even in case of a point load $f(x, y) = \delta(x, y)$ the function w will be smooth with respect to space variables because of the smoothing properties of the operator K^{-1}. This justifies making use of the system (3.9)–(3.10) even for the load concentrated at a point. It is worth to notice that this advantageous property is achieved by keeping rotary inertia in the viscoelastic Bernoulli Eq. (2.4) that is usually neglected by other authors. Thus there is no need for regularization of the point load. It is smoothed naturally in our framework by the inverse operator K^{-1}.

4. Exact solutions of linearized problems

As mentioned above, for flexural-gravity waves due to moving loads under regular operating conditions, it is usually sufficient to consider the linearized problem. In the case when the load is moving at a constant speed, these linearized equations can then be solved *exactly*.

We introduce the operators

$$R = \frac{bG_0}{2\rho K}, \quad Q = \frac{g\varkappa\Delta^2}{K},$$

$$U = \sqrt{\frac{g(1 + \varkappa D^4)G_0}{K} - R^2},$$

and denote the corresponding Fourier symbols by the same letters $R(\xi)$, $Q(\xi)$ and $U(\xi)$. Clearly, these symbols are strictly positive for $\xi \neq 0$ and equal zero at $\xi = 0$. Note that we also include the situation $b = 0$ and so $R = 0$ for any frequency. Below, we solve the linearized systems using the Laplace transformation $\mathcal{L}$. Let $\widehat{\eta}$, $\widehat{\Phi}$ and $\widehat{w}$ be Laplace transforms of η, Φ and w. The latter has the transform

$$\widehat{w}(x, y, s) = \frac{1}{(2\pi)^2}\int_{\mathbb{R}^2}\frac{e^{i(x-x_0)\xi_1+iy\xi_2}\widehat{f}(\xi_1, \xi_2)}{(s + i\xi_1 v)K(\xi_1, \xi_2)}d\xi_1 d\xi_2. \tag{4.1}$$

For the initial values we use notations $\eta_0 = \eta(t = 0)$, $\Phi_0 = \Phi(t = 0)$.

4.1. Zhestkaya problem [23]

In this case $\mathcal{Q} = \varkappa g\Delta^2(1 + \tau_f\partial_t)$ and the linearized system has the form

$$\eta_t = G_0\Phi, \tag{4.2}$$

$$\Phi_t = -(R^2 + U^2)G_0^{-1}\eta - (2R + \tau_f QG_0)\Phi - w. \tag{4.3}$$

This system transforms to

$$\widehat{\eta}(s) = \frac{1}{d(s)}\left\{(s + 2R + \tau_f QG_0)\eta_0 + G_0\Phi_0 - G_0\widehat{w}(s)\right\},$$

$$\widehat{\Phi}(s) = \frac{1}{d(s)}\left\{-(R^2 + U^2)G_0^{-1}\eta_0 + s\Phi_0 - s\widehat{w}(s)\right\}$$

with the denominator $d(s) = s^2 + (2R + \tau_f Q G_0)s + R^2 + U^2$. Introducing the symbols $\alpha(\xi) = \sqrt{R^2 + U^2}$ and $\beta(\xi) = R + \tau_f Q G_0/2$ one can rewrite the denominator as $d(s) = (s+\beta)^2 + \alpha^2 - \beta^2$. The roots $s_1 = -\beta - \sqrt{\beta^2 - \alpha^2}$ and $s_2 = -\beta + \sqrt{\beta^2 - \alpha^2}$ define the dynamical behaviour of the system. For the damping symbol, we have $\beta(\xi) > 0$ provided $\xi \neq 0$ and either $b \neq 0$ or $\tau_f \neq 0$. On the other hand, we have $\alpha(\xi) = 0$ if and only if $\xi = 0$. As a result the system is stable: $\Re s_{1,2} < 0$. A simple analysis shows that $\alpha(\xi) \sim \sqrt{gH}|\xi|$ and $\beta(\xi) \sim \frac{bH}{2\rho}|\xi|^2$ as $|\xi| \to 0$. Thus $s_{1,2}(\xi) \sim \mp i\sqrt{gH}|\xi|$ as $|\xi| \to 0$. Similarly $\alpha(\xi) \sim \sqrt{\frac{E}{\rho_1(1-\nu^2)}}|\xi|$ and $\beta(\xi) \sim \frac{\tau_f E}{2\rho_1(1-\nu^2)}|\xi|^2$ as $|\xi| \to \infty$.

The solution of this system has the form $\eta(t) = \mathcal{S}_{11}(t)\eta_0 + \mathcal{S}_{12}(t)\Phi_0 + \eta^w(t)$ and $\Phi(t) = \mathcal{S}_{21}(t)\eta_0 + \mathcal{S}_{22}(t)\Phi_0 + \Phi^w(t)$ where the terms η^w, Φ^w are due to the external force:

$$\eta^w(t) = \mathcal{L}^{-1}\left(\frac{-G_0}{d(s)}\widehat{w}(s)\right), \quad \Phi^w(t) = \mathcal{L}^{-1}\left(\frac{-s}{d(s)}\widehat{w}(s)\right)$$

and

$$\mathcal{S}_{11} = \frac{s_2 e^{s_1 t} - s_1 e^{s_2 t}}{s_2 - s_1}, \quad \mathcal{S}_{12} = \frac{G_0\left(e^{s_1 t} - e^{s_2 t}\right)}{s_1 - s_2},$$
$$\mathcal{S}_{21} = \frac{\alpha^2\left(e^{s_1 t} - e^{s_2 t}\right)}{G_0(s_2 - s_1)}, \quad \mathcal{S}_{22} = \frac{s_1 e^{s_1 t} - s_2 e^{s_2 t}}{s_1 - s_2}.$$

And so we have

$$\eta^w(x,y,t) = \mathcal{F}^{-1}\left(A_\eta(\xi)e^{s_1 t} + B_\eta(\xi)e^{s_2 t} + C_\eta(\xi)e^{-i\xi_1 v t}\right)(x - x_0, y),$$

$$\Phi^w(x,y,t) = \mathcal{F}^{-1}\left(A_\Phi(\xi)e^{s_1 t} + B_\Phi(\xi)e^{s_2 t} + C_\Phi(\xi)e^{-i\xi_1 v t}\right)(x - x_0, y),$$

where the symbols corresponding to the ice sheet deformation are

$$A_\eta(\xi) = \frac{\widehat{f}(\xi)K(\xi)^{-1}G_0(\xi)}{(s_2(\xi) - s_1(\xi))(s_1(\xi) + i\xi_1 v)},$$
$$B_\eta(\xi) = \frac{\widehat{f}(\xi)K(\xi)^{-1}G_0(\xi)}{(s_1(\xi) - s_2(\xi))(s_2(\xi) + i\xi_1 v)},$$
$$C_\eta(\xi) = -\frac{\widehat{f}(\xi)K(\xi)^{-1}G_0(\xi)}{(s_1(\xi) + i\xi_1 v)(s_2(\xi) + i\xi_1 v)}$$

and the symbols corresponding to the trace of the velocity potential are

$$A_\Phi(\xi) = \frac{\widehat{f}(\xi)K(\xi)^{-1}s_1(\xi)}{(s_2(\xi) - s_1(\xi))(s_1(\xi) + i\xi_1 v)},$$
$$B_\Phi(\xi) = \frac{\widehat{f}(\xi)K(\xi)^{-1}s_2(\xi)}{(s_1(\xi) - s_2(\xi))(s_2(\xi) + i\xi_1 v)},$$
$$C_\Phi(\xi) = \frac{\widehat{f}(\xi)K(\xi)^{-1}i\xi_1 v}{(s_1(\xi) + i\xi_1 v)(s_2(\xi) + i\xi_1 v)}.$$

These formulae represent the exact solution of the system (4.2)–(4.3). In addition, numerical implementation is straightforward. One can see that functions under the inverse Fourier transform are continuous and fast decreasing with respect to ξ. Note that the fundamental matrix operator $\mathcal{S}$ satisfies the group property $\mathcal{S}(t_1 + t_2) = \mathcal{S}(t_1)\mathcal{S}(t_2)$. This operator together with the symbols $A_\eta(\xi)$, $B_\eta(\xi)$ and $A_\Phi(\xi)$, $B_\Phi(\xi)$ are overdamped by exponents $\exp(s_{1,2}t)$ after a short time. As a result the main part of the solution is due to $C_\eta(\xi)$ and $C_\Phi(\xi)$. However, these symbols are singular at $\xi = 0$ and their inverse Fourier transform is not even defined. On the other hand approximating the exponents linearly one can see that for small frequencies $A_\eta(\xi)e^{s_1 t} + B_\eta(\xi)e^{s_2 t} + C_\eta(\xi)e^{-i\xi_1 v t} \approx 0$ and $A_\Phi(\xi)e^{s_1 t} + B_\Phi(\xi)e^{s_2 t} + C_\Phi(\xi)e^{-i\xi_1 v t} \approx -t\widehat{f}(\xi)K(\xi)^{-1}$. The meaning of the first identity is conservation of fluid mass $\int \eta dxdy = \int \eta_0 dxdy$. The second identity tells us that $\int \Phi dxdy$ is proportional to time t which is in line with the fact that a potential is always defined up to a nonphysical constant. So one should not discard exponentially decreasing symbols $A_\eta(\xi)$, $B_\eta(\xi)$ since their appearance guarantees good behaviour near zero $\xi = 0$ of the function standing under the inverse Fourier transform, in particular they provide its continuity. Though in practical calculations after discretization of the problem one can exclude zero-harmonics and the symbols A_η and B_η together. The same is true for $\Phi(x,y,t)$.

Finally, one should notice that even though these symbols are continuous when it comes to numerical evaluation of the integrals there may be problems if some grid points are close to the relation $s_2(\xi) = s_1(\xi)$. If $s_2 = s_1$ then

$$\mathcal{S}_{11} = (1 - s_1 t)e^{s_1 t}, \quad \mathcal{S}_{12} = G_0 t e^{s_1 t},$$

$$\mathcal{S}_{21} = \alpha^2 G_0^{-1} t e^{s_1 t}, \quad \mathcal{S}_{22} = (1 + s_1 t)e^{s_1 t}$$

and

$$A_\eta(\xi)e^{s_1 t} + B_\eta(\xi)e^{s_2 t} = \frac{\widehat{f}(\xi)G_0(\xi)(1-(s_1(\xi)+i\xi_1 v)t)e^{s_1 t}}{K(\xi)(s_1(\xi)+i\xi_1 v)^2},$$

$$A_\Phi(\xi)e^{s_1 t} + B_\Phi(\xi)e^{s_2 t} = -\frac{\widehat{f}(\xi)(i\xi_1 v + (s_1(\xi)+i\xi_1 v)s_1 t)e^{s_1 t}}{K(\xi)(s_1(\xi)+i\xi_1 v)^2}.$$

4.2. Hosking problem [25]

In this case $\mathcal{Q}\eta = \varkappa g \Delta^2 \left(\eta - \int_0^\infty \Psi(\tau)\eta(t-\tau)d\tau\right)$ and the system has the form

$$\eta_t = G_0\Phi, \tag{4.4}$$

$$\Phi_t = -(R^2+U^2)G_0^{-1}\eta + Q\int_0^\infty \Psi(\tau)\eta(t-\tau)d\tau - 2R\Phi - w. \tag{4.5}$$

The hereditary integral is defined via the memory function

$$\Psi(t) = \sum_{j=0}^{n} A_j e^{-\alpha_j t} \tag{4.6}$$

where $A_j > 0$ and $\alpha_j > 0$ are the viscoelastic parameters. In what follows we regard the particular case

$$\Psi(t) = Ae^{-\alpha t}. \tag{4.7}$$

Note that $A \leqslant \alpha$ if we assume $\int_0^\infty \Psi(\tau)d\tau \leqslant 1$ which is a natural physical condition. The hereditary integral is the sum of the convolution of the memory function Ψ with the ice sheet deflection η and the remainder $I(t) = \int_t^\infty \Psi(\tau)\eta(t-\tau)d\tau$. Assuming that the load was at rest for a long time before starting to move, i.e. $\eta(t) \equiv \eta_0$ for all $t \leqslant 0$, and accepting the simplest memory function (4.7) we can calculate explicitly $I(t) = \eta_0 Ae^{-\alpha t}/\alpha$.

Applying the Laplace transform to the system (4.4)–(4.5), we obtain

$$\widehat{\eta}(s) = \frac{1}{(s+R)^2+U^2-G_0Q\widehat{\Psi}(s)}\left((s+2R)\eta_0 + G_0\Phi_0 - G_0\widehat{w}(s) + G_0Q\widehat{I}(s)\right),$$

$$\widehat{\Phi}(s) = \frac{1}{(s+R)^2+U^2-G_0Q\widehat{\Psi}(s)}\left((Q\widehat{\Psi}(s) - (R^2+U^2)G_0^{-1})\eta_0 + s\Phi_0 - s\widehat{w}(s) + sQ\widehat{I}(s)\right),$$

where so far we have not applied any assumptions on the memory function Ψ and the values of elevation for negative time. Taking the general view of the memory function (4.6) we arrive at rational functions with respect to s. For the partial-fractions decomposition, one has to find roots of the corresponding denominator. This can be done numerically without any difficulties with an arbitrary *a priory* accuracy on a frequency grid used for spatial discretization of the problem. However, in the simplest case (4.7) one can find those roots analytically. Indeed, with the memory function (4.7) and condition $\eta(t) \equiv \eta_0$ for negative t, we have $\widehat{\Psi}(s) = \frac{A}{s+\alpha}$, $\widehat{I}(s) = \frac{A\eta_0}{\alpha(s+\alpha)}$ and the system in s-domain has the form

$$\widehat{\eta}(s) = \frac{1}{d(s)}\left((s^2+2Rs+\alpha s+2R\alpha+G_0QA/\alpha)\eta_0 + (s+\alpha)G_0\Phi_0 - (s+\alpha)G_0\widehat{w}(s)\right),$$

$$\widehat{\Phi}(s) = \frac{s+\alpha}{d(s)}\left((QA/\alpha - (R^2+U^2)G_0^{-1})\eta_0 + s\Phi_0 - s\widehat{w}(s)\right),$$

with the denominator $d(s) = ((s+R)^2+U^2)(s+\alpha) - G_0QA$. We denote the roots by $s_{1,2,3}(\xi)$. It is easy to see that the same equations can be rewritten as

$$\widehat{\eta}(s) = \frac{1}{d(s)}\left((s^2-(s_1+s_2+s_3)s+s_1s_2+s_2s_3+s_1s_3+s_1s_2s_3/\alpha)\eta_0\right.$$
$$\left.+(s+\alpha)G_0\Phi_0 - (s+\alpha)G_0\widehat{w}(s)\right),$$

$$\widehat{\Phi}(s) = \frac{s+\alpha}{d(s)}\left(\frac{s_1s_2s_3}{\alpha G_0}\eta_0 + s\Phi_0 - s\widehat{w}(s)\right).$$

Explicit formulae for the roots $s_{1,2,3}(\xi)$ can be obtained using symbolic software without any problem, but since these formulae are cumbersome, we omit the exact expressions here. Obviously, there is at least one root $s_1(\xi) < 0$ for any value of ξ. For $\xi = 0$, we keep $s_2(0) = s_3(0) = 0$. Otherwise, as long as the physical condition $\alpha \geqslant A$ holds true, the Routh–Hurwitz stability criterion guarantees stability of the system $\Re s_{2,3} < 0$. It is difficult to say something more about the roots in general. However, it turns out that in practical physical conditions all these roots are different. More precisely, their imaginary parts $\Im s_1(\xi) = 0$, $\Im s_2(\xi) > 0$ and $\Im s_3(\xi) < 0$ provided $\xi \neq 0$ (see below).

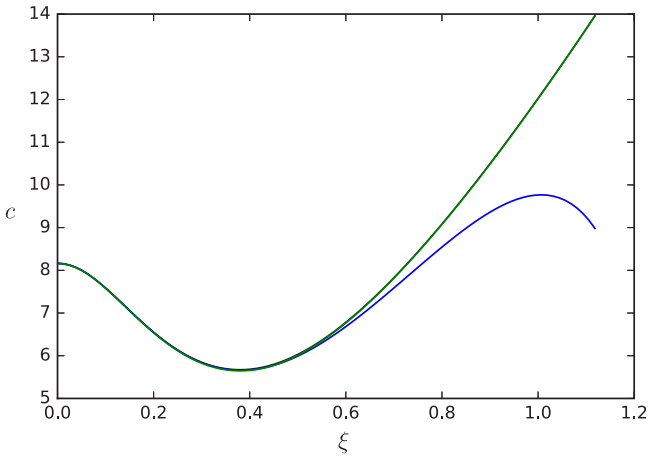

Fig. 1. Dispersion relations $c(\xi)$. The colour coding is as follows: blue – Zhestkaya model; green – Hosking model; black – $c_0(\xi)$ without damping (almost indistinguishable from Hosking model). (For interpretation of the references to colour in this figure legend, the reader is referred to the web version of this article.)

For each index $i \in \{1, 2, 3\}$, we introduce the operator

$$S_i(t) = \frac{(s_i + \alpha)e^{s_i t}}{(s_i - s_j)(s_i - s_k)} \text{ with different } j, k \in \{1, 2, 3\} \setminus \{i\}.$$

As in the previous case, the solution $\eta(t)$, $\Phi(t)$ can be represented via the fundamental matrix operator

$$\mathcal{S}_{11} = \frac{1}{\alpha}(s_2 s_3 S_1 + s_1 s_3 S_2 + s_1 s_2 S_3), \quad \mathcal{S}_{12} = G_0(S_1 + S_2 + S_3),$$

$$\mathcal{S}_{21} = \frac{s_1 s_2 s_3}{\alpha G_0}(S_1 + S_2 + S_3), \quad \mathcal{S}_{22} = s_1 S_1 + s_2 S_2 + s_3 S_3,$$

and

$$\eta^w(x, y, t) = \mathcal{F}^{-1}\left(A_\eta(\xi, t) + C_\eta(\xi)e^{-i\xi_1 v t}\right)(x - x_0, y),$$

$$\Phi^w(x, y, t) = \mathcal{F}^{-1}\left(A_\Phi(\xi, t) + C_\Phi(\xi)e^{-i\xi_1 v t}\right)(x - x_0, y)$$

where the symbols corresponding to the deflection are

$$A_\eta(\xi, t) = -\frac{\widehat{f}(\xi)G_0(\xi)}{K(\xi)}\left(\frac{S_1(\xi, t)}{s_1(\xi) + i\xi_1 v} + \frac{S_2(\xi, t)}{s_2(\xi) + i\xi_1 v} + \frac{S_3(\xi, t)}{s_3(\xi) + i\xi_1 v}\right),$$

$$C_\eta(\xi) = \frac{\widehat{f}(\xi)G_0(\xi)(\alpha - i\xi_1 v)}{K(\xi)(s_1(\xi) + i\xi_1 v)(s_2(\xi) + i\xi_1 v)(s_3(\xi) + i\xi_1 v)}$$

and the symbols corresponding to the velocity potential are

$$A_\Phi(\xi, t) = -\frac{\widehat{f}(\xi)}{K(\xi)}\left(\frac{s_1(\xi)S_1(\xi, t)}{s_1(\xi) + i\xi_1 v} + \frac{s_2(\xi)S_2(\xi, t)}{s_2(\xi) + i\xi_1 v} + \frac{s_3(\xi)S_3(\xi, t)}{s_3(\xi) + i\xi_1 v}\right),$$

$$C_\Phi(\xi) = -\frac{\widehat{f}(\xi)i\xi_1 v(\alpha - i\xi_1 v)}{K(\xi)(s_1(\xi) + i\xi_1 v)(s_2(\xi) + i\xi_1 v)(s_3(\xi) + i\xi_1 v)}.$$

5. Results and discussion

We will present some profiles of the solutions for the two viscoelastic cases considered here. For calculations we have used physical parameters close the ones given in [6]. More exactly, the gravitational acceleration is $g = 9.8$ m/s^2, the water depth $H = 6.8$m, the ice thickness $h = 0.17$m, the water density $\rho = 1026$kg/m^3, the ice density $\rho_1 = 917$kg/m^3 and the action radius $L_\varkappa = \sqrt[4]{\varkappa} = 2$m. Following Takizawa [6] we define the critical damping coefficient as $b_c = 2\sqrt{\rho g \rho_1 h}$. We set the relative rough damping $b/b_c = 0.2$, the strain-relaxation time $\tau_f = 0.1s$, the viscoelastic memory parameters $A = 0.4$ and $\alpha = 0.5$. The load has the mass 235kg with the length 2.43 m and the width 0.79 m. In fact, this load can be well approximated by a concentrated load, as the numerical results will not change significantly if one assumes the

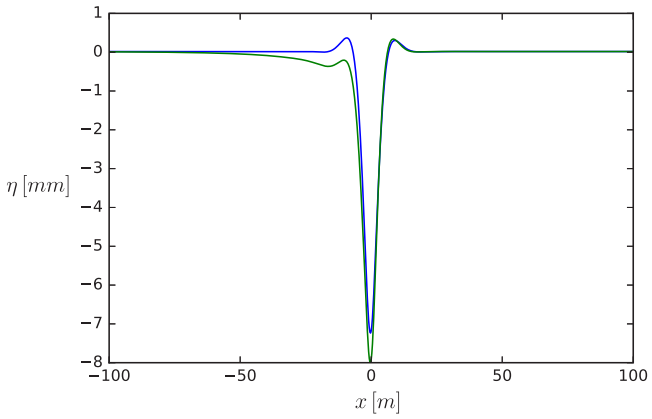

Fig. 2. Displacement in the case $v = 3$ m/s. The colour coding is as follows: blue — Zhestkaya system; green — Hosking system. (For interpretation of the references to colour in this figure legend, the reader is referred to the web version of this article.)

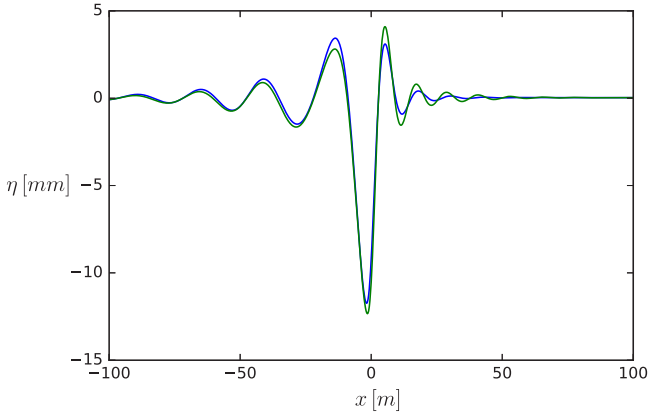

Fig. 3. Displacement in case $v = 6$ m/s. The colour coding is as follows: blue — Zhestkaya system; green — Hosking system. (For interpretation of the references to colour in this figure legend, the reader is referred to the web version of this article.)

weight to be a δ-function. This is because the size of the truck is negligible compared with the flexural waves it excites in the ice sheet [8]

The dependence of the phase speed c on the wave number ξ of free flexural waves is known as the dispersion relation. Without any damping, i.e. with $b = 0$, $\tau_f = 0$, $A = 0$ the dispersion relation is given by

$$c_0(\xi) = \sqrt{g(1 + \varkappa|\xi|^4)\frac{\tanh(H|\xi|)}{|\xi|K(\xi)}}.$$

By the dispersion relation for viscoelastic models we understand the expression

$$c(\xi) = \Im s_2(\xi)/|\xi|,$$

where it is supposed in the notation for the roots that the imaginary part is $\Im s_2(\xi) \geqslant 0$. We plot these dispersion relations in Fig. 1. The first local minimum is approximately 5.7 m/s, which is close to the critical velocity 5.8 m/s given in [6].

We plot some solutions for velocities below this minimum (Fig. 2), between this minimum and the long-wave velocity $\sqrt{gH} = 8.2$ m/s (Fig. 3) and higher than the long-wave velocity (Fig. 4). The load is located at $x = 0$ and moves to the right. Only the centreline (the x-axis) is shown here. The type of solution changes, depending on the velocity of the load. For low velocities, there is only a localized response of the ice sheet near the moving load. For the Hosking system the asymmetry is more pronounced, with the rim behind the load being lower than the one in front.

In the second example (Fig. 3) two trains of waves with different wavelengths are visible, in front and behind the load. The waves behind the load are longer than the ones in front of the load. One can observe the lag between the load and the minimum depression. The waves travelling in front of the load predicted by the Hosking system have higher amplitudes than the one predicted by Zhestkaya system for our choice of parameters.

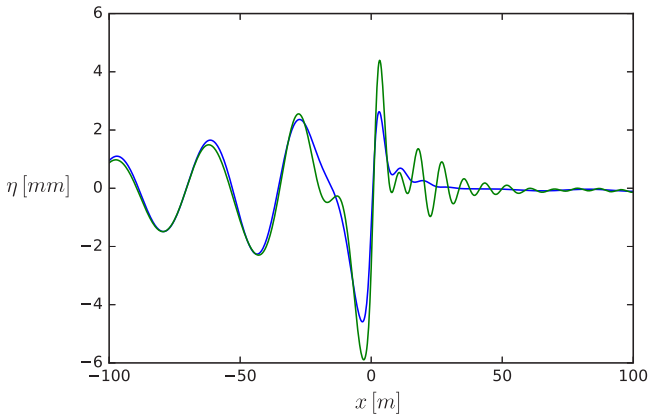

Fig. 4. Displacement in case $v = 9$ m/s. The colour coding is as follows: blue — Zhestkaya system; green — Hosking system. (For interpretation of the references to colour in this figure legend, the reader is referred to the web version of this article.)

In conclusion, we have obtained new exact solutions for two different viscoelastic formulations of the problem of a load moving on a floating ice plate. Laplace transforms were used to derive these exact solutions. Some examples have been presented for various values of the parameters. The load was assumed to be rectangular, but due to the inclusion of rotary inertia and the scale separation between the load and the wavelength of the excited waves, a point load could also be used.

CRediT authorship contribution statement

Evgueni Dinvay: Conceptualization, Methodology, Investigation, Software, Writing – original draft, Writing – review & editing. **Henrik Kalisch:** Conceptualization, Writing – review & editing, Funding acquisition. **Emilian Părău:** Conceptualization, Writing – review & editing, Funding acquisition.

Declaration of competing interest

The authors declare that they have no known competing financial interests or personal relationships that could have appeared to influence the work reported in this paper.

Acknowledgements

This research was supported by the Research Council of Norway under grant no. 239033/F20. E.P. has been partially supported by the EPSRC under grant EP/J019305/1. The authors would like to thank the Isaac Newton Institute for Mathematical Sciences and the University of Cambridge for support and hospitality during the programme Mathematics of sea ice phenomena where work on this paper was undertaken (EPSRC grant no. EP/K032208/1 and Simons Foundation).

Appendix

As calculations with data provided by Takizawa [6] show, all three zeroes $s_{1,2,3}$ are different in the case of the Hosking model. Thus the following limit formulae are given only the sake of completeness. If $s_2 = s_3$ then

$$\mathcal{S}_{11} = \frac{1}{\alpha}\left(s_2 s_3 S_1 + s_1 e^{s_2 t}\left(\frac{\alpha s_1 - 2\alpha s_2 - s_2^2}{(s_1 - s_2)^2} - \frac{(s_2+\alpha)s_2 t}{s_1 - s_2}\right)\right),$$

$$\mathcal{S}_{12} = G_0\left(S_1 - e^{s_2 t}\left(\frac{s_1+\alpha}{(s_1 - s_2)^2} + \frac{(s_2+\alpha)t}{s_1 - s_2}\right)\right),$$

$$\mathcal{S}_{21} = \frac{s_1 s_2^2}{\alpha G_0}\left(S_1 - e^{s_2 t}\left(\frac{s_1+\alpha}{(s_1 - s_2)^2} + \frac{(s_2+\alpha)t}{s_1 - s_2}\right)\right),$$

$$\mathcal{S}_{22} = s_1 S_1 - e^{s_2 t}\left(\frac{\alpha s_1 + 2 s_1 s_2 - s_2^2}{(s_1 - s_2)^2} + \frac{(s_2+\alpha)s_2 t}{s_1 - s_2}\right),$$

$$A_\eta(\xi, t) = -\frac{\widehat{f}(\xi) G_0(\xi)}{K(\xi)}\left(\frac{S_1(\xi, t)}{s_1(\xi) + i\xi_1 v} - \widetilde{A}_\eta(\xi) e^{s_2 t}\right),$$

$$A_\Phi(\xi,t) = -\frac{\widehat{f}(\xi)}{K(\xi)}\left(\frac{s_1(\xi)S_1(\xi,t)}{s_1(\xi)+i\xi_1 v} - \widetilde{A}_\Phi(\xi)e^{s_2 t}\right),$$

with

$$\widetilde{A}_\eta(\xi) = \frac{i\xi_1 v(s_1+\alpha) - \alpha s_1 + 2\alpha s_2 + s_2^2}{(s_1-s_2)^2(s_2(\xi)+i\xi_1 v)^2} + \frac{(s_2+\alpha)t}{(s_1-s_2)(s_2(\xi)+i\xi_1 v)},$$

$$\widetilde{A}_\Phi(\xi) = \frac{i\xi_1 v(\alpha s_1 + 2s_1 s_2 - s_2^2) + (s_1+\alpha)s_2^2}{(s_1-s_2)^2(s_2(\xi)+i\xi_1 v)^2} + \frac{(s_2+\alpha)s_2 t}{(s_1-s_2)(s_2(\xi)+i\xi_1 v)}$$

If $s_1 = s_2 = s_3$ then

$$\mathcal{S}_{11} = \left(1 - s_1 t + \frac{(s_1+\alpha)s_1^2 t^2}{2\alpha}\right)e^{s_1 t}, \quad \mathcal{S}_{12} = \left(1 + \frac{(s_1+\alpha)t}{2}\right)G_0 t e^{s_1 t},$$

$$\mathcal{S}_{21} = \left(1 + \frac{(s_1+\alpha)t}{2}\right)\frac{s_1^3 t e^{s_1 t}}{\alpha G_0}, \quad \mathcal{S}_{22} = \left(1 + (2s_1+\alpha)t + \frac{(s_1+\alpha)s_1 t^2}{2}\right)e^{s_1 t}$$

and

$$A_\eta(\xi,t) = \frac{\widehat{f}(\xi)G_0(\xi)e^{s_1 t}}{K(\xi)}\left(\frac{i\xi_1 v - \alpha}{(s_1(\xi)+i\xi_1 v)^3} - \frac{(i\xi_1 v - \alpha)t}{(s_1(\xi)+i\xi_1 v)^2} - \frac{(s_1+\alpha)t^2}{2(s_1(\xi)+i\xi_1 v)}\right),$$

$$A_\Phi(\xi,t) = -\frac{\widehat{f}(\xi)e^{s_1 t}}{K(\xi)}\left(\frac{i\xi_1 v(i\xi_1 v - \alpha)}{(s_1(\xi)+i\xi_1 v)^3} + \frac{(s_1^2 + 2i\xi_1 v s_1 + i\xi_1 v\alpha)t}{(s_1(\xi)+i\xi_1 v)^2} + \frac{(s_1+\alpha)s_1 t^2}{2(s_1(\xi)+i\xi_1 v)}\right).$$

References

[1] G.D. Ashton, River and Lake Ice Engineering, Water Resources Publications, Littleton, Colorado, 1986.
[2] V.A. Squire, R.J. Hosking, A.D. Kerr, P.J. Langhorne, Moving Loads on Ice Plates, Vol. 45, Springer Science & Business Media, 2012.
[3] A. Korobkin, E.I. Părău, J.-M. Vanden-Broeck, The mathematical challenges and modelling of hydroelasticity, Phil. Trans. Roy. Soc. London A 369 (2011) 2803–2812.
[4] R. Romeyn, A. Hanssen, B.O. Ruud, T.A. Johansen, Elastic properties of floating sea ice from air-coupled flexural waves, Cryosphere Discuss. (2021) 1–25.
[5] V.A. Squire, Ocean wave interactions with sea ice: A reappraisal, Annu. Rev. Fluid Mech. 52 (2020) 37–60.
[6] T. Takizawa, Field studies on response of a floating sea ice sheet to a steadily moving load, Contrib. Inst. Low Temp. Sci. A 36 (1987) 31–76.
[7] T. Takizawa, Response of a floating sea ice sheet to a steadily moving load, J. Geophys. Res. 93 (1988) 5100–5112.
[8] J.W. Davys, R.J. Hosking, A.D. Sneyd, Waves due to a steadily moving source on a floating ice plate, J. Fluid Mech. 158 (1985) 269–287.
[9] A.V. Pogorelova, Wave resistance of an air-cushion vehicle in unsteady motion over an ice sheet, J. Appl. Mech. Tech. Phys. 49 (2008) 71–79.
[10] I.V. Sturova, Motion of a load over an ice sheet with non-uniform compression, Fluid Dyn. 56 (2021) 503–512.
[11] E. Dinvay, H. Kalisch, E.I. Părău, Fully dispersive models for moving loads on ice sheets, J. Fluid Mech. 876 (2019) 122–149.
[12] R.J. Hosking, F. Milinazzo, The response of a floating ice sheet to a line load moving at variable speed, J. Fluid Mech. 938 (2022).
[13] A.A. Matiushina, A.V. Pogorelova, V.M. Kozin, Effect of impact load on the ice cover during the landing of an airplane, Internat. J. Offshore Polar Eng. 26 (2016) 6–12.
[14] I.V. Sturova, Unsteady three-dimensional sources in deep water with an elastic cover and their applications, J. Fluid Mech. 730 (2013) 392–418.
[15] H. Babaei, J. Van der Sanden, N. Short, P. Barrette, Lake ice cover deflection induced by moving vehicles: Comparing theoretical results with satellite observations, in: TAC 2016: Efficient Transportation-Managing the Demand-2016 Conference and Exhibition of the Transportation Association of Canada.
[16] A.V. Marchenko, Damping of surface waves propagating below solid ice, in: The 26th International Ocean and Polar Engineering Conference, ISOPE, 2016.
[17] E.I. Părău, F. Dias, Nonlinear effects in the response of a floating ice plate to a moving load, J. Fluid Mech. 460 (2002) 281–305.
[18] P. Aceves-Sánchez, A.A. Minzoni, P. Panayotaros, Numerical study of a nonlocal model for water-waves with variable depth, Wave Motion 50 (2013) 80–93.
[19] D. Moldabayev, H. Kalisch, D. Dutykh, The Whitham equation as a model for surface water waves, Physica D 309 (2015) 99–107.
[20] G.B. Whitham, Variational methods and applications to water waves, Proc. R. Soc. Lond. Ser. A 299 (1967) 6–25.
[21] E. Dinvay, H. Kalisch, D. Moldabayev, E.I. Părău, The Whitham equation for hydroelastic waves, Appl. Ocean Res. 89 (2019) 202–210.
[22] V.M. Kozin, A.V. Pogorelova, Effect of the viscosity properties of ice on the deflection of an ice sheet subjected to a moving load, J. Appl. Mech. Tech. Phys. 50 (2009) 484–492.
[23] V.D. Zhestkaya, Numerical solution of the problem of an ice sheet under a moving load, J. Appl. Mech. Tech. Phys. 40 (1999) 770–775.
[24] D.E. Kheisin, Ice Cover Dynamics [in Russian], Gidrometeoizdat, Leningrad, 1967.
[25] R.J. Hosking, A.D. Sneyd, D.W. Waugh, Viscoelastic response of a floating ice plate to a steadily moving load, J. Fluid Mech. 196 (1988) 409–430.
[26] K. Wang, R.J. Hosking, F. Milinazzo, Time-dependent response of a floating viscoelastic plate to an impulsively started moving load, J. Fluid Mech. 521 (2004) 295–317.
[27] J.R. Marko, Observations and analyses of an intense waves-in-ice event in the Sea of Okhotsk, J. Geoph. Res. 108 (2003) 3296.
[28] D.P. Nicholls, F. Reitich, A new approach to analyticity of Dirichlet-Neumann operators, Proc. Roy. Soc. Edinburgh Sect. A 131 (2001) 1411–1433.